Influence of Microstructure on Dynamic Mechanical Behaviour of Polymeric Composites with Complex Inclusions

K. R. KIM, J. H. AN,* K. W. CHO, and C. E. PARK

Research Institute of Industrial Science and Technology, P.O. Box 135, Pohang, 790-600, Korea

SYNOPSIS

The dynamic mechanical properties of polymeric composites composed of crosslinked poly(*n*-butyl methacrylate) continuous-phase and crosslinked polystyrene dispersed phase with poly(*n*-butyl methacrylate) occlusion have been examined. The composite samples were prepared by mixing and swelling of the crosslinked polystyrene particles obtained by emulsifier-free emulsion polymerization, with *n*-butyl methacrylate and crosslinker, then photopolymerizing at the desired temperature. The composite microstructure was varied by either changing the crosslink density of polystyrene, and temperature of swelling and polymerization, or using different sizes and contents of polystyrene particles. The tan δ peak positions of composite samples are found to be dependent on morphological characteristics as well as the properties of the dispersed phase while the peak height seems to be dependent on the effective volume of dispersed phase composed of polystyrene and poly(*n*-butyl methacrylate) occlusions. Special attention has been paid to the comparison among composite, homonetworks, and bulk IPN samples that are expected to have the identical structure with the complex dispersed phase of the composite samples. © 1993 John Wiley & Sons, Inc.

INTRODUCTION

Dynamic mechanical characterization is a tool of major importance for the study of polymer blends and composites since the variation of properties is conveniently determined as a function of temperature and frequency. The investigation of the dynamic modulus and loss factors over a wide range of temperatures has been used to evaluate the miscibility,[1-4] interface,[5-7] damping characteristics,[8,9] and morphological variation.[10-12]

Although dynamic mechanical spectra may provide a conclusive basis for the distinction between compatible and incompatible blends,[13,14] a complication can arise in analyzing phase separated blends or composites since the mechanical response of multiphase materials is dependent not only on the nature of constituents but also on the physical or structural arrangement of phases such as morphology and interface. These factors are often closely interrelated and cannot be treated independently.

The effect of interface is often exemplified in the particulate or fiber-filled polymer composites, where the presence of a hard filler phase results in modification of matrix glass transition. The shift in its temperature either toward higher or lower temperature has been noted experimentally.[6,15,16] These features are usually interpreted as a result of variation in the properties of the interface between filler and matrix. In the extreme case where a strong interaction exists between fiber and matrix resin,[17,18] a new relaxation peak at a temperature higher than the glass transition of the matrix phase has been observed, which has been considered to be the glass transition of a hypothetical interface consisting of

* To whom correspondence should be addressed at Department of Chemical Engineering, Pohang Institute of Science and Technology, P.O. Box 125, Pohang, 790-600, Korea.

Journal of Applied Polymer Science, Vol. 47, 305–322 (1993)
 CCC 0021-8995/93/020305-18

the matrix chains anchoring on the surface of fillers. A similar observation has been reported in the case of polymer blends such as the polystyrene/polycarbonate pair,[19] in which a composition-independent transition in between those of PC and PS appears and is attributed to the intermixing of two components with subsequent creation of an interface.

In conflict with this three-phase model is an alternative explanation in which such a change in the glass transition of each component or appearance of a new transition can be explained as consequences of the overall behaviour of a two-phase system such as morphology and phase continuity without assuming the presence of interface.[20–22] In addition to the contributions of interface and morphology that are clearly interrelated, the possible presence of bulk miscibility between components makes the interpretation of dynamic mechanical spectra more complicated in the case of polymer blends.

Both theoretical and experimental attempts have been made for the analysis of dynamic mechanical properties of multi-phase materials. Various types of theoretical equations have been developed for the prediction of properties of constituents.[23–25] Caville et al.[26,27] have compared the dynamic mechanical behaviour of polymer films made from latices by different emulsion processes and discussed them in relation to particle morphologies. Guest et al.[28] have examined PC/SANS blends prepared from two different procedures: compression molding and injection molding. The major differences in spectra were attributed to morphological differences. One of the most interesting features in terms of morphology would be the case with complex inclusion such as HIPS and ABS. Dickie[29] has calculated the dynamic mechanical response of a particulate composite with complex inclusion based on the Kerner equation. As predicted in Dickie's model calculation, the modulus and tan δ of HIPS were experimentally found to be dependent on the effective volume fraction of dispersed phase rather than the content of rubber.[30,31]

The objective of this paper is to investigate the dynamic mechanical response in the composite sample consisting of a continuous rubbery phase and dispersed plastic phase containing occlusions of rubbery component. By varying the content or the properties of the dispersed phase, and the amount of rubbery occlusion in the dispersed plastic phase, the influence of microstructure is studied. Special attention has been paid to the comparison of dynamic mechanical behaviour of the composite sample and the dispersed complex domain itself that is prepared separately.

EXPERIMENTAL

Preparation of Composite Samples

The samples containing complex inclusions were prepared by the following procedure as shown in Figure 1:

1. Prepare the crosslinked polystyrene (PS) particle by emulsifier free emulsion polymerization.
2. The dried polystyrene emulsion particles were mixed with an excess amount of monomer mixture containing *n*-butyl methacrylate, crosslinker and initiator.
3. The mixture containing PS particles was kept in a sealed container at the desired temperature until the equilibrium amount of monomer mixture was swelled into the particles.
4. Finally, the mixture was poured into glass molds and placed in a UV reactor in which the temperature was controlled at the same temperature as that of the swelling step.

The styrene monomer was purified by distillation and potassium persulphate as received was used as the initiator in the emulsifier-free emulsion polymerization. The crosslink density was varied by the amount of divinyl benzene (DVB) added to the styrene monomer. The particle size was controlled by changing the polymerization temperature and reaction time. Polymerization conditions and average particle size data are given in Table I.

The prepared emulsion product was dried in a vacuum oven at 60°C for 3 days. The dried emulsion particles were mixed with an excess amount of the monomer mixture composed of *n*-butyl methacrylate (BMA), tetraethylene glycol dimethacrylate (TEGDM), and benzoin as a photoinitiator. The mixture was kept at 0°C or 40°C until the equilibrium amount of monomer mixture was swelled into the PS particles. The swelled mixture was placed in between two glass plates using silicon gaskets. A metal frame is then placed in each side of the "sandwich" and the cell is clamped with small spring-loaded clamps to follow the shrinkage during the polymerization. The sample cell was placed between two UV sources (12 Watt, 365 nm high pressure mercury lamp) in order to ensure uniform irradiation and polymerized for 1 or 2 days in the box, in which the temperature was kept the same as the swelling temperature. The polymerized sample was vacuum dried and cut into a rectangular shape for dynamic mechanical analysis.

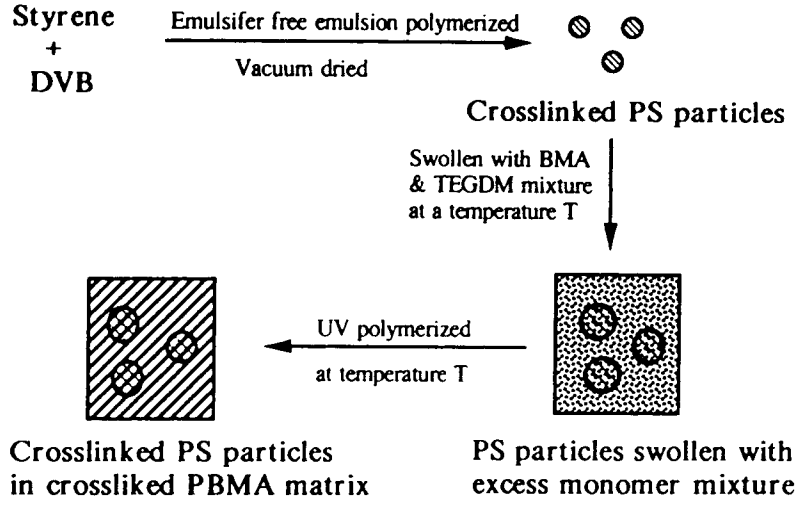

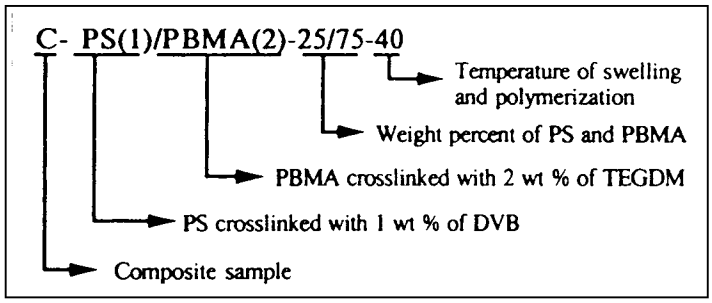

Figure 1 Preparation procedure and notation for the composite samples.

The composite samples prepared in this manner are designated as "C" series and the meaning of each abbreviation is shown in Figure 1.

Preparation of PS and PBMA Homonetworks

In order to estimate the size of PS complex domains in the final composite samples, it is necessary to measure the crosslink density of PS particles and the degree of swelling at each temperature. The crosslink density was estimated by measuring the degree of swelling with the bulk size of homonetwork composed of styrene and DVB that was prepared separately. The PS homonetworks were prepared in exactly the same manner as in the composite sample preparation except that a slight excess of DVB was required to match the glass transition temperature of homonetwork with that of corresponding PS par-

Table I Preparation of Crosslinked Polystyrene Emulsion Particles

Sample I.D.	PS-1	PS-2	PS-5	PS-2′	PS-2″
Styrene (g/L)[a]	10.395	10.29	9.975	10.29	10.29
DVB (g/L)[a]	0.105	0.21	0.525	0.21	0.21
Potassium persulfate (g/L)[a]	1.892	1.892	1.892	1.892	1.892
Reaction temperature (°C)	70	70	70	100	60
Reaction time (hour)	8	8	8	2	24
Average particle size (μm)	0.5	0.5	0.5	0.17	1.30
Glass transition temp. (°C)[b]	105.2	107.9	115	107.7	107.8

[a] Based on water.
[b] Determined by DSC.

ticles determined by DSC. The PBMA homonetworks composed of *n*-butyl methacrylate and tetraethylene glycol dimethacrylate were also prepared for comparison. The homonetworks sample were designated as "H" series and the sample preparation procedure and notations are summarized in Figure 2.

Preparation of Bulk PS-PBMA IPNs

The disperse phase of the composite samples would have a multi-phase structure composed of polystyrene network and poly(*n*-butyl acrylate) network, which could be considered as a small-scale sequential type of interpenetrating polymer networks (IPN) that is synthesized by swelling crosslinked polymer I in monomer II, then subsequently polymerized and crosslinked. Since the separate characterization of the disperse phase alone is impossible, macroscopic samples of sequential IPN composed of the same species were separately prepared as shown in Figure 3. Starting with a PS homonetwork of which the glass transition was matched with corresponding PS particles, an equilibrium amount of BMA and TEGDM mixture was allowed to swell into the homonetwork. After equilibrium, the excess monomer mixture was removed and photopolymerized in exactly the same manner as the preparation of composite sample.

Dynamic Mechanical Analysis

E', E'', and tan δ for the samples were measured using a Polymer Laboratories Dynamic Mechanical Thermal Analyzer interfaced with Compaq PC. Dynamic mechanical spectra were obtained in the single cantilever bending mode following the standard techniques under the following conditions: a scan rate of 2°C/min, a frequency of 1 Hz, and a temperature range from −30 to 160°C. The sample for measurement was cut into a piece 3.0 × 11.0 × 5 mm.

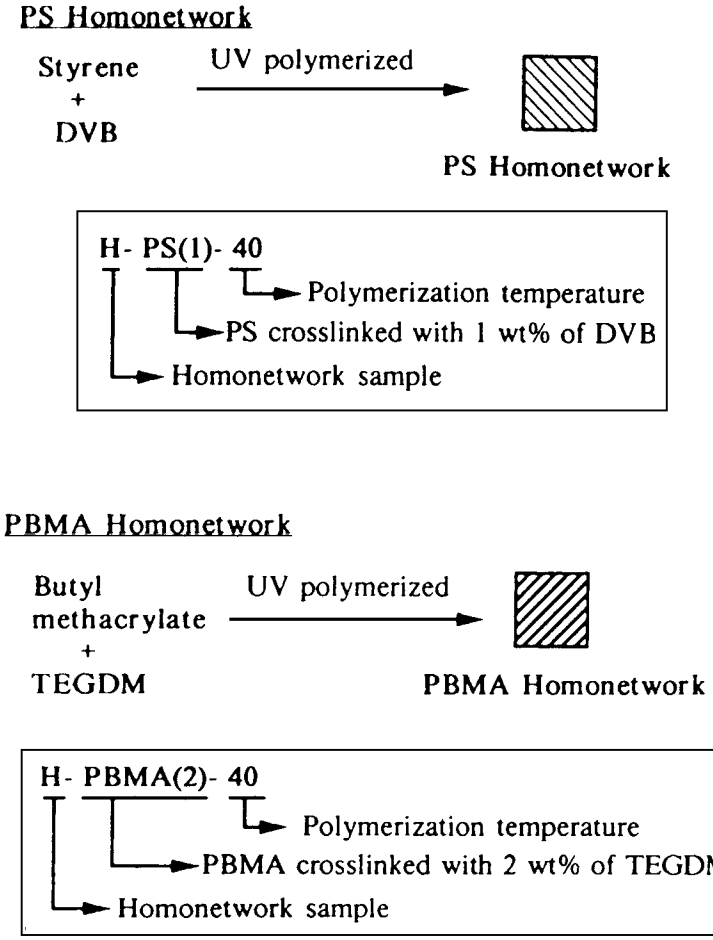

Figure 2 Preparation procedure and notation for the homonetwork samples.

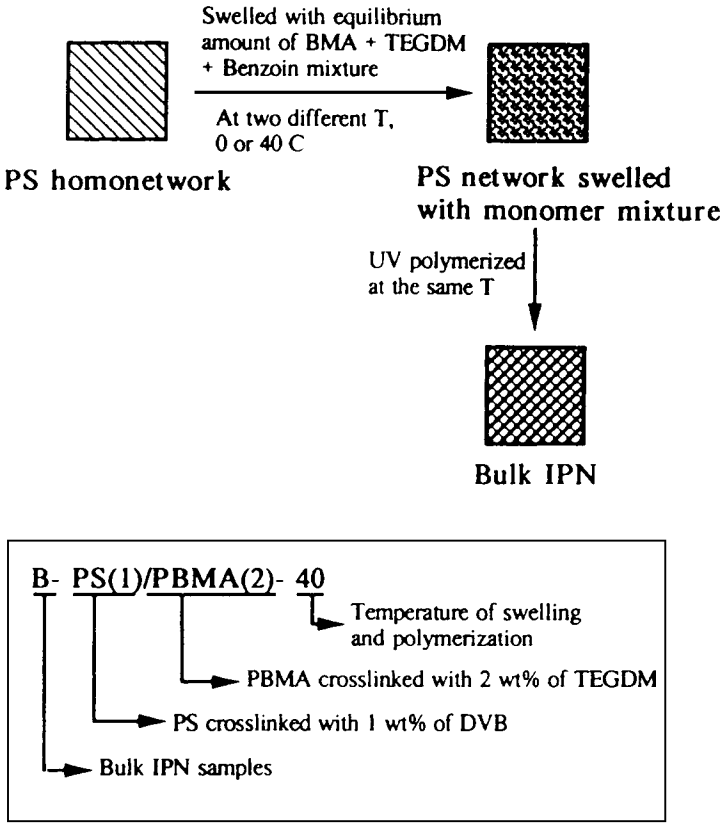

Figure 3 Preparation procedure and notation for the bulk IPN samples.

Other Characterization

Latex particle-size analysis was performed on a Malvern Zetasizer model IIc at a temperature of 25°C and a refractive index of 1.33. The glass transition temperatures of some samples were analyzed using a Perkin–Elmer DSC 7 with a heating rate of 20°C/min. The midpoint of the transition region was taken as the glass transition point. In order to check the dispersion of PS particles in a composite sample, the surface of a fractured sample in liquid nitrogen was observed with scanning electron microscopy (SEM).

RESULTS AND DISCUSSION

The overall morphology of the composite sample is illustrated in SEM microphotographs of the fractured surface shown in Figure 4. These microphotographs indicate that the polystyrene particles retain their spherical shapes and are relatively well distributed.

From the sample preparation procedure, it is obvious that the effective volume of dispersed phase is dependent on how much acrylic monomer is swelled into crosslinked PS particles. Since the direct determination of the effective volume in a composite form is rather difficult, we measured the degree of swelling with the polystyrene homonetwork of which the glass transitions were matched with those of the corresponding PS particles. The swelling measurements were performed with *n*-butyl methacrylate monomer at 0°C and 40°C and the results are summarized in Table II. Based on these data, the effective volume of dispersed phase in the composite samples is estimated in the further discussion.

Effect of Particle Contents

Figures 5 and 6 present the tan δ, and modulus behaviour of the composite samples with different loadings of PS particles, in which the low temperature transition region corresponds to PBMA, and the high temperature one is characteristic of PS-rich dispersed phase. Since the crosslink density of particles and the swelling and polymerization temperature are the same for all samples, the size and properties of individual domains could be regarded as being identical. The peak height is highly depen-

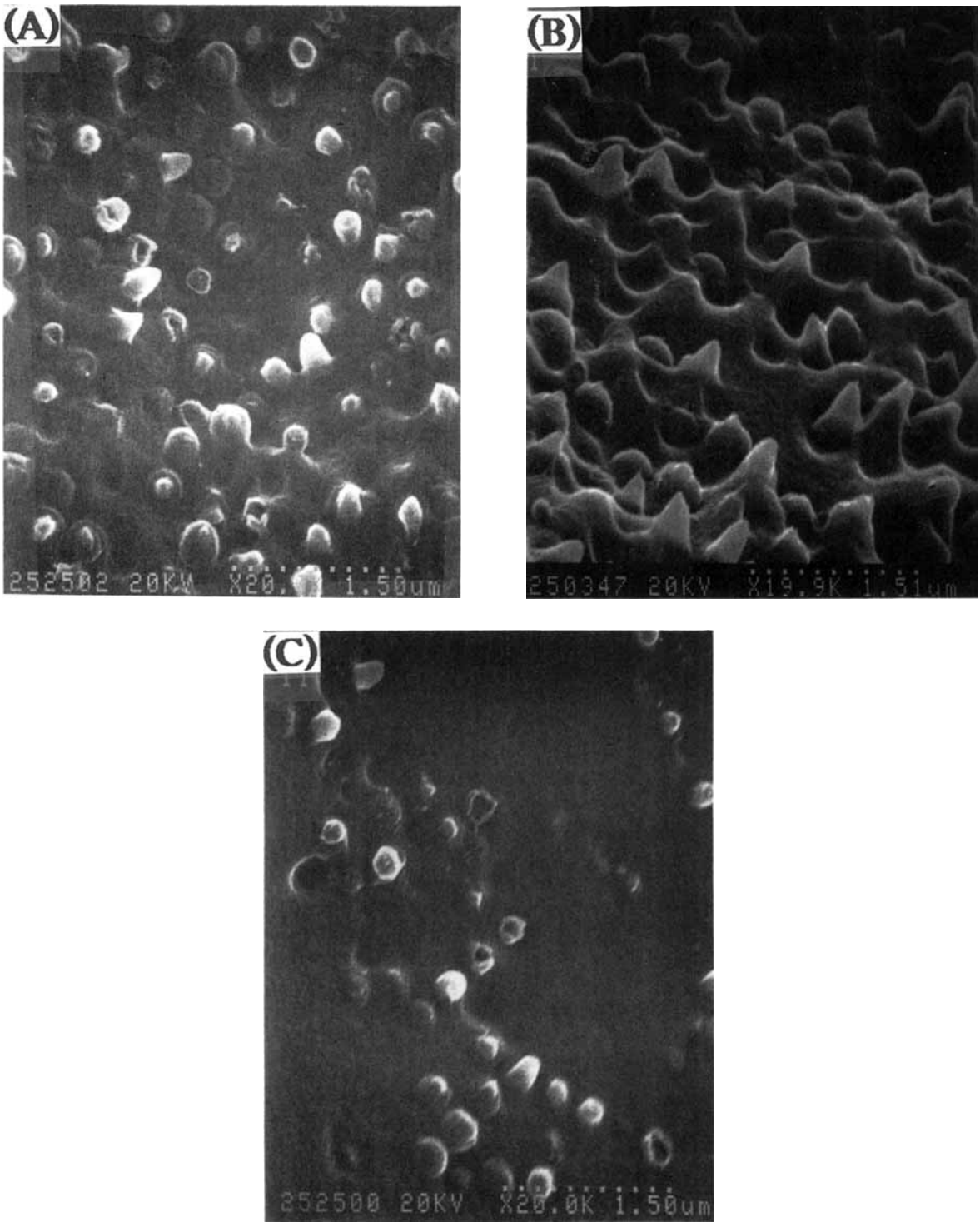

Figure 4 SEM microphotographs of liquid nitrogen fractured surface of composite samples. (A): C-PS(2)/PBMA(2)-25/75-40; (B): C-PS(2)/PBMA(2)-15/85-40; (C): C-PS(2)/PBMA(2)-5/95-40.

dent on the volume fraction of each phase while the peak position of PS does not show much variation with particle contents since the effective volume fraction of the dispersed phase is varied from 46 to 9.2% (see Table III). However, there is a slight shift toward a higher temperature in the position of

Table II Properties of Polystyrene Homonetworks

Sample I.D.	Volumetric Swelling Ratio[a] 40°C	Volumetric Swelling Ratio[a] 0°C	Glass Transition Temperature[b] (°C)
H-PS(1)-40	1.84	1.04	105.7
H-PS(2)-40	1.72	1.03	107.7
H-PS(5)-40	1.14	1.02	115.8

[a] With *n*-butyl methacrylate at each temperature.
[b] Determined by DSC before swelling.

PBMA tan δ peak with increasing PS particle contents, which can be confirmed by the modulus behavior shown in Figure 6. This trend is in agreement with the model calculation done by Dickie,[29] in which an increase in peak height of the dispersed phase was observed with increasing volume fraction of the dispersed phase. However, the peak position of the PS-rich dispersed phase seems to be invariant in contrast to the model calculation in which the peak position of the dispersed phase also showed phase-volume dependency. The difference between the current sample and the model is that the model calculation assumes that the effective volume of dispersed phase including occlusion is varied while the overall composition of rubbery and glassy component is fixed. Therefore, the properties of complex inclusion itself varied as well as the effective volume fraction of the dispersed phase. In contrast, the properties of the complex inclusions are kept constant in this series of samples since the crosslink density and the swelling degree would be the same for each sample, which seems to be reflected in the invariance of the peak position of the dispersed phase with particle contents.

Similar results were obtained in another set of samples synthesized at 0°C as shown in Figure 7. Therefore, it is suggested that the increase or decrease in the volume fraction of dispersed phase does not affect the peak position for the dispersed phase very much, if the properties of the dispersed phase are not changed, while the position of the continuous phase tan δ shows a weak dependency on the PS particle loading.

Effect of Crosslink Density of the Polystyrene Particle

When the crosslink density of PS particles is varied, it may affect the properties of the composite sample in several ways. First, the total amount of acrylate monomer mixture swelled into the PS particles will be decreased as the crosslink density of PS particles is increased, which in turn reduces the effective vol-

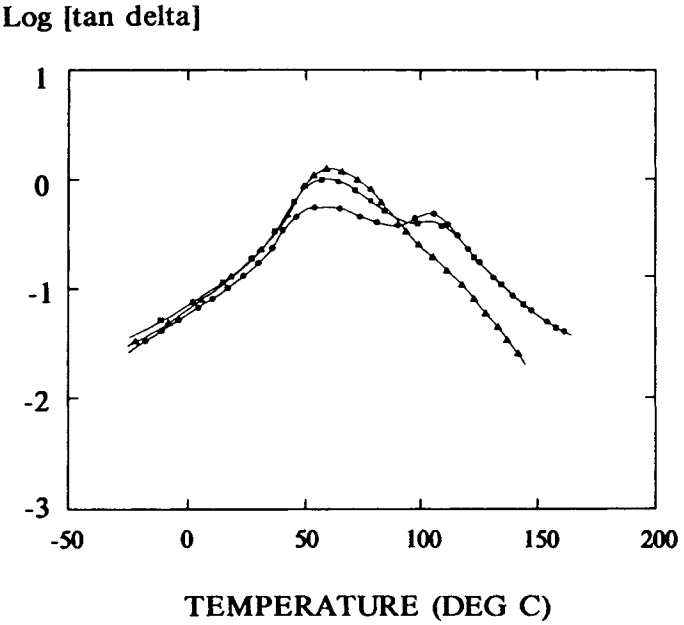

Figure 5 Effect of PS particle contents on tan δ of composite sample while fixing crosslink density and temperature. (●): C-PS(1)/PBMA(2)-25/75-40; (■): C-PS(1)/PBMA(2)-15/85-40; (▲): C-PS(1)/PBMA(2)-5/95-40.

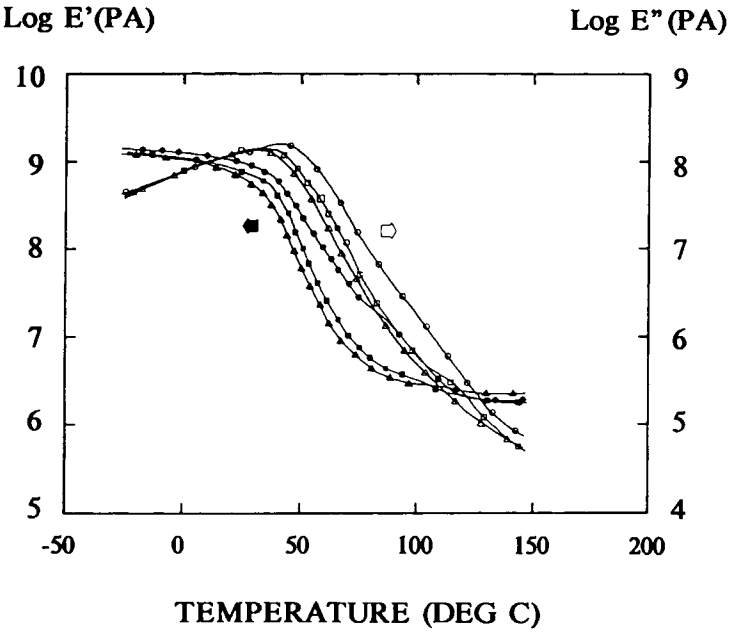

Figure 6 Effect of PS particle contents on modulus of composite sample while fixing crosslink density and temperature. (●): C-PS(1)/PBMA(2)-25/75-40; (■): C-PS(1)/PBMA(2)-15/85-40; (▲): C-PS(1)/PBMA(2)-5/95-40.

ume fraction of disperse phase composed of the polystyrene network and PBMA subinclusion upon polymerization of acrylic monomer. Secondly, as often observed in many IPN studies, the introduction of crosslinks restricts the progress of phase separation, which is often manifested in a reduced domain size or shape,[32] a broadened transition peak, and/or an inwared shift of each constituent's T_g depending on the degree of miscibility between them.[33,34] Therefore, it also affects the properties of the dispersed phase itself.

In Figure 8, tan δ versus temperature plots of three different composite samples are shown that have identical overall composition and polymerization conditions except for the crosslink density of PS particles. Table III shows the effective volume fractions of the PS-rich dispersed phases in the composite samples, which are calculated based on

Table III Volume Fractions of Each Phase in Composite Samples Calculated Based on the Swelling Ratio in Table II

Sample I.D.	Apparent Volume Fraction		Effective Volume Fraction		
	PS	PBMA	Continuous Phase[a]	Dispersed Phase[b]	Occlusion[c]
C-PS(5)/PBMA(2)-15/75-40	0.15	0.85	0.829	0.171	0.021
C-PS(2)/PBMA(2)-15/85-40	0.15	0.85	0.742	0.258	0.108
C-PS(1)/PBMA(2)-15/85-40	0.15	0.85	0.724	0.276	0.126
C-PS(1)/PBMA(2)-15/85-0	0.15	0.85	0.844	0.156	0.006
C-PS(5)/PBMA(2)-25/75-40	0.25	0.75	0.715	0.285	0.035
C-PS(2)/PBMA(2)-25/75-40	0.25	0.75	0.570	0.430	0.180
C-PS(1)/PBMA(2)-25/75-40	0.25	0.75	0.540	0.460	0.210
C-PS(1)/PBMA(2)-25/75-0	0.25	0.75	0.740	0.260	0.010
C-PS(1)/PBMA(2)-5/95-40	0.5	0.95	0.908	0.092	0.042

[a] Fraction of PBMA present in the matrix.
[b] Fraction of complex PS domains including PBMA occlusions.
[c] Fraction of PBMA present as occlusions inside of complex PS domains.

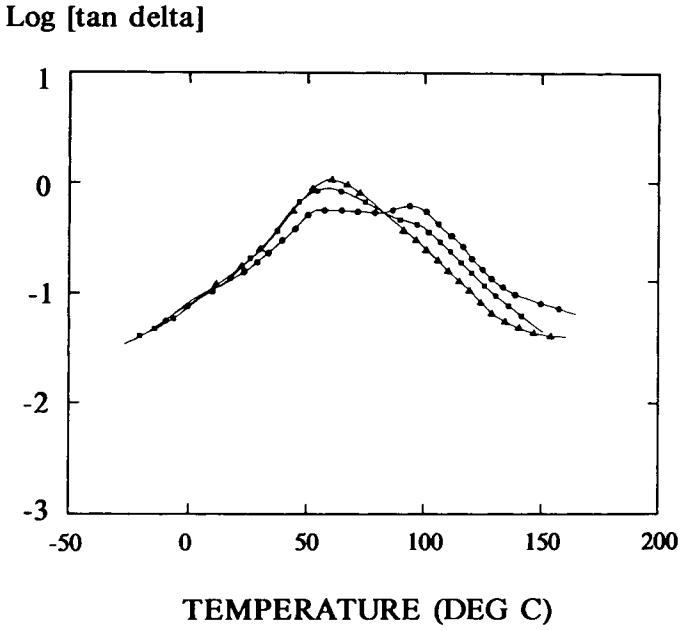

Figure 7 Effect of PS particle contents on tan δ of composite sample while fixing crosslink density and temperature. (●): C-PS(1)/PBMA(2)-25/75-0; (■): C-PS(1)/PBMA(2)-15/85-0; (▲): C-PS(1)/PBMA(2)-5/95-0.

the swelling data of homonetwork in Table II. Sample, C-PS5/PBMA2-40, which is expected to have the smallest effective disperse-phase volume fraction including acrylic occlusions inside the PS domains, shows the smallest height of the PS transition peaks among the three. On the contrary, the peak height of PBMA transitions seems to be decreasing relatively as the crosslink density decreases. This feature indicates that the peak height is dependent on the effective volume of dispersed phase rather than the

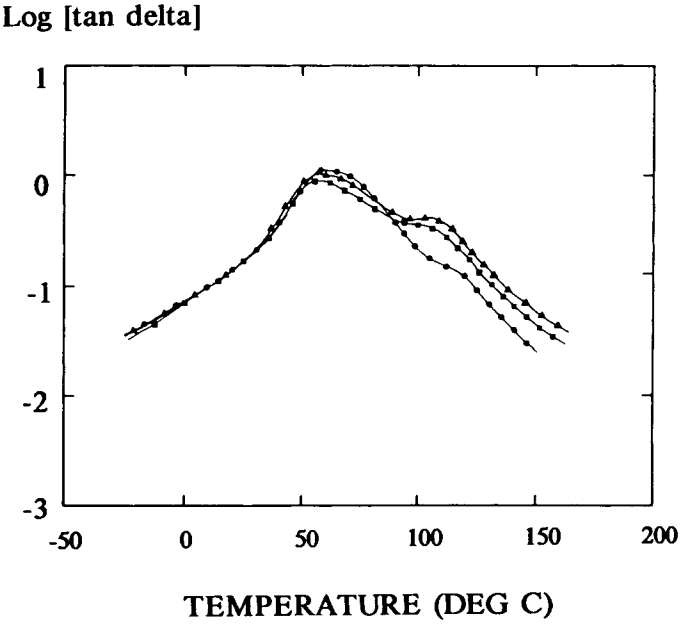

Figure 8 Effect of PS crosslink density on tan δ of composite sample while fixing particle content and temperature. (●): C-PS(5)/PBMA(2)-15/85-40; (■): C-PS(2)/PBMA(2)-15/85-40; (▲): C-PS(1)/PBMA(2)-15/85-40.

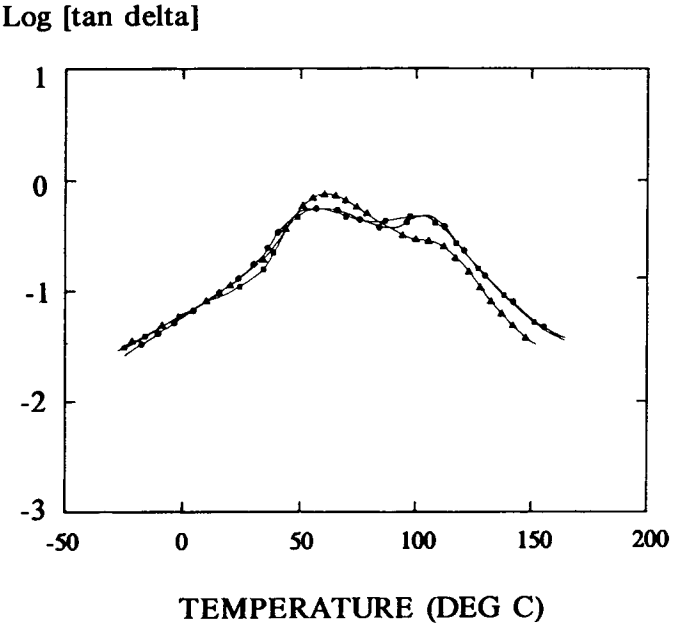

Figure 9 Effect of PS crosslink density on tan δ of composite sample while fixing particle content and temperature. (●): C-PS(1)/PBMA(2)-25/75-40; (■): C-PS(2)/PBMA(2)-25/75-40; (▲): C-PS(5)/PBMA(2)-25/75-40.

overall composition. The change of peak height in PBMA loss peak seems to be relatively marginal compared with that of the PS disperse phase consistent with the model calculation by Dickie,[25] where the continuous phase loss tan δ was less phase-volume dependent than the dispersed one. The composite samples with higher content of PS particles yielded similar results as is shown in Figure 9.

When comparing peak positions, both PS and PBMA transitions were found to shift to higher temperature with an increase in the crosslink density of PS particle as shown in Figures 8 and 9. The shift of PS transition peaks toward higher temperatures seems to be the consequence of the increase in the crosslink density of PS components. However, the position of each peak is found to be significantly different from that of the corresponding PS homonetwork or bulk IPN as discussed in the next section, which suggests that it is also somewhat associated with the morphological characteristics. In the case of the PBMA peak shifts, only a marginal difference was observed among samples. Since the majority of PBMA components are still present outside the dispersed domains as a continuous phase, the molecular level interaction between PS and PBMA component seems to be less. Therefore, the shift of PBMA tan δ should be attributed to the matrix-dispersed phase interaction, combined with the change in the properties of dispersed phase itself.

The variation of loss and storage modulus with temperature for the composite samples is shown in Figure 10. As expected from the sample preparation procedure, the storage moduli of composite samples tend to lie closer to that of PBMA homonetwork reflecting the continuity of PBMA component. Here, it is worthwhile to note that the modulus level in the rubbery plateau region increases with increasing crosslink density of PS component even though the effective volume of the dispersed phase decreases as the crosslink density of PS component increases. On the other hand, the change in the effective volume of the dispersed phase did not cause much variation in the rubbery plateau modulus when the crosslink density of PS component was kept constant (Fig. 6).

Comparison with Bulk IPNs

It is of interest to compare the behaviour of the composite samples with that of the bulk IPN samples since the bulk IPNs can be considered to represent the properties of the complex domain of the composite sample in large scale. Dynamic mechanical spectra of bulk IPN samples given in Figure 11 show two distinct transition peaks indicating the immiscibility of this system. Also the storage modulus behaviour indicates the continuity of PS component. As in the composite sample, tan δ peak

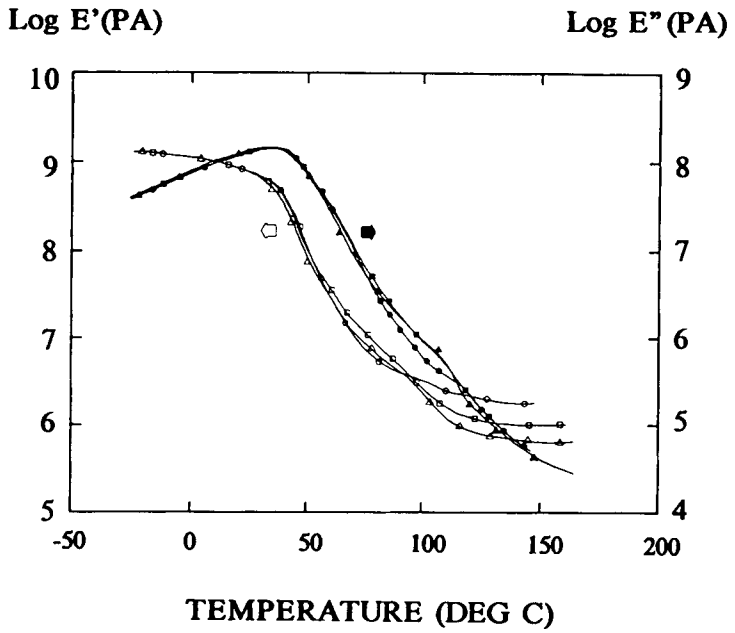

Figure 10 Effect of PS crosslink density on modulus of composite sample while fixing particle content and temperature. (●): C-PS(5)/PBMA(2)-15/85-40; (■): C-PS(2)/PBMA(2)-15/85-40; (▲): C-PS(1)/PBMA(2)-15/85-40.

height depends on the volume fraction of each constituent (volume fractions are shown in Table IV). When the PS transition peaks in bulk IPNs are compared with those of the corresponding homonetworks (Fig. 12), the peak positions and broadness are found to be almost identical for both cases, which indicates that there is no noticeable change in polystyrene phase even upon formation of IPN.

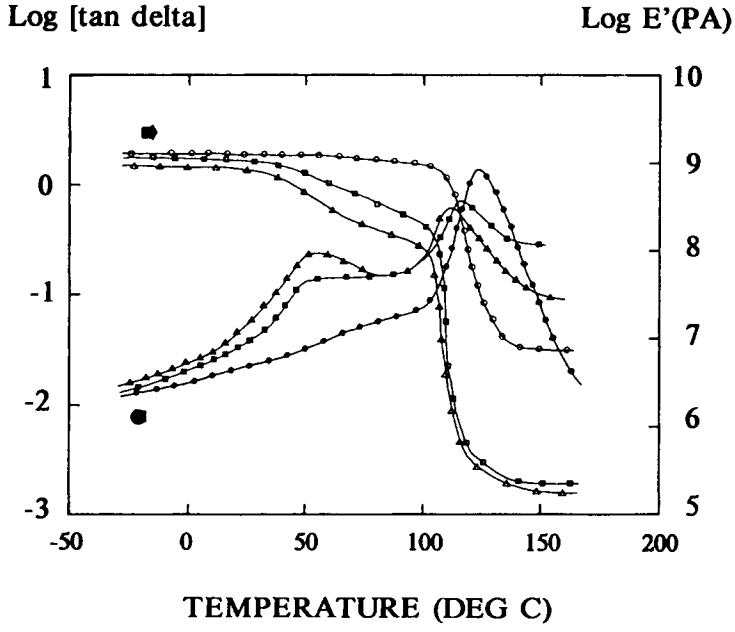

Figure 11 Modulus and tan delta of bulk IPN samples made from PS networks with three different crosslink density. (●): B-PS(5)/PBMA(2)-40; (■): B-PS(2)/PBMA(2)-40; (▲): B-PS(1)/PBMA(2)-40.

Table IV Volume Fraction of Each Phase in Bulk IPN Samples

Sample I.D.	Volume Fraction PS	PBMA
B-PS(1)/PBMA(2)-40	0.543	0.457
B-PS(2)/PBMA(2)-40	0.581	0.419
B-PS(5)/PBMA(2)-40	0.877	0.123
B-PS(1)/PBMA(2)-0	0.961	0.039
B-PS(2)/PBMA(2)-0	0.971	0.029
B-PS(5)/PBMA(2)-0	0.980	0.02

However, the PBMA loss peaks in all bulk IPN samples are shifted down about 8° in temperature relative to that of the PBMA homonetwork. This feature again indicates that there is no apparent miscibility enhancement by IPN formation that is often manifested by inward shifts of constituents' glass transitions. Such a downshift of rubbery inclusion's transition in glassy continuous samples has been noted by several authors investigating ABS, HIPS, and block copolymers,[35-37] which was explained on the basis of negative pressure upon cooling by the mismatch of thermal expansion coefficients. But, this seems to be incorrect in our case, since the temperature employed in the sample preparation is 40°C, which is quite near room temperature. Another possible explanation would be via the model calculation of simple rubber inclusion case by Dickie,[29] in which a downward shift of the dispersed phase-loss maximum was explained by the strong dependency on the ratio of matrix and dispersed phase-storage moduli and the degree of shift increased with the volume fraction of dispersed phase. The third possibility would be the possible effect of interphase, in which a shift toward lower temperature is considered as an indication of bad adhesion. This is less likely in our sample since it is generally expected that the interface is rather secure due to the interpenetration effect of IPNs. However, we do not have enough information to make a judgement on the detailed cause of such shifts. The only conclusion from this observation is that the shift may relate more to morphological difference than the molecular level miscibility change upon IPN formation.

When we compared the tan δ among four different samples including composite, bulk IPN, PBMA homonetwork, and PS homonetwork (Figs. 13–15), the PS tan δ maximum of composite sample appears at 5–10°C lower than that of bulk IPN or the homonetwork sample. On the other hand, in the case of PBMA tan δ, the composite sample shows its transition peak in between those of bulk IPN and PBMA homonetwork. The most obvious difference between composite and bulk IPN samples would be in their morphology. Above all, the polystyrene phase shows macroscopic continuity throughout the sample in

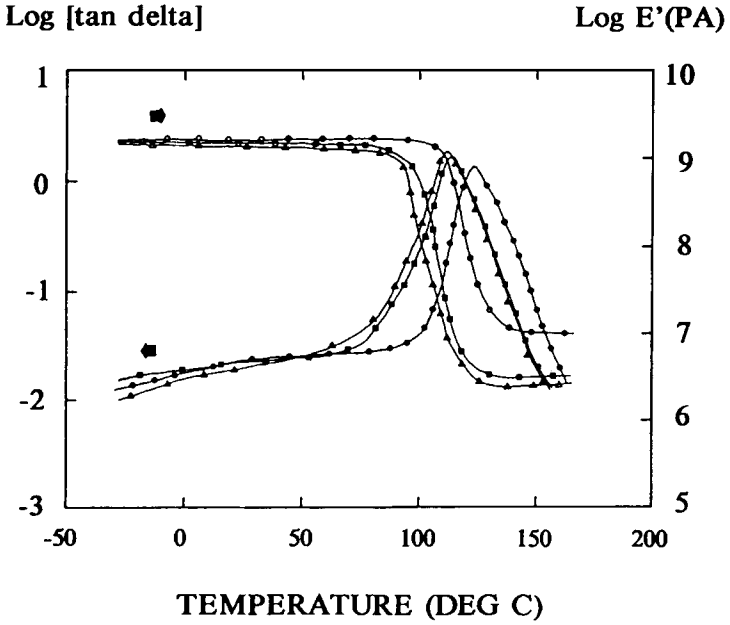

Figure 12 Modulus and tan delta of PS homonetwork with three different crosslink density. (●): H-PS(5)-40; (■): H-PS(2)-40; (▲): H-PS(1)-40.

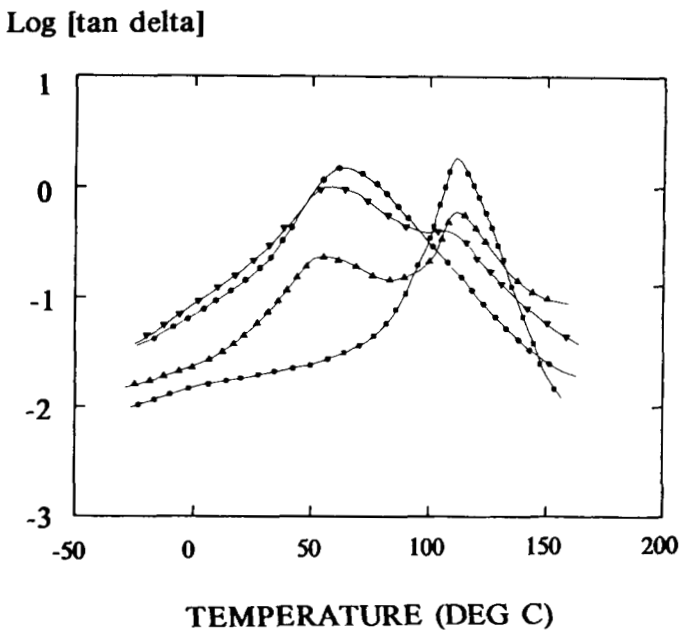

Figure 13 Comparison of tan delta behaviour among composite, bulk IPN, PS homonetwork, and PBMA homonetwork samples. (■): H-PS(1)-40; (▲): B-PS(1)/PBMA(2)-40; (▼): C-PS(1)/PBMA(2)-15/85-40; (●): H-PBMA(2)-40.

bulk IPN. On the other hand, each PS-rich domain of the composite sample forms a discrete phase even though there is a continuity of PS phase in the individual PS-rich dispersed domains. Also, in contrast to composites containing inert fillers, the PBMA subinclusion in the PS domains may have some degree of connectivity with the matrix phase, which may affect the nature of interface between matrix and dispersed phase in the composite samples.

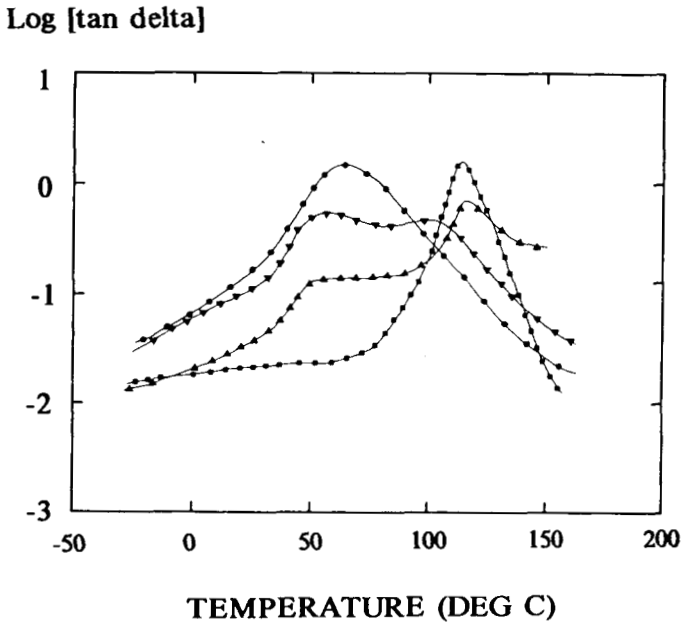

Figure 14 Comparison of tan delta behaviour among composite, bulk IPN, PS homonetwork, and PBMA homonetwork samples. (■): H-PS(2)-40; (▲): B-PS(2)/PBMA(2)-40; (▼): C-PS(2)/PBMA(2)-25/75-40; (●): H-PBMA(2)-40.

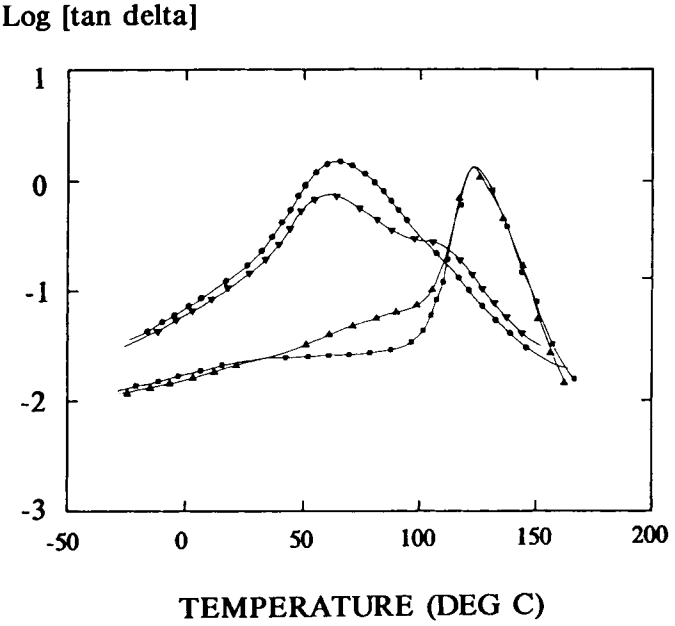

Figure 15 Comparison of tan delta behaviour among composite, bulk IPN, PS homonetwork, and PBMA homonetwork samples. (■): H-PS(5)-40; (▲): B-PS(5)/PBMA(2)-40; (▼): C-PS(5)/PBMA(2)-25/75-40; (●): H-PBMA(2)-40.

Effect of Swelling and Polymerization Temperature

When we change the temperature of swelling and polymerization at fixed crosslink density of PS particles, the amount of acrylic subinclusion into the PS particles is affected as shown in Table III. Figures 16 and 17 show the tan δ behaviour of composite samples synthesized at two different temperatures for two sets of samples with different overall com-

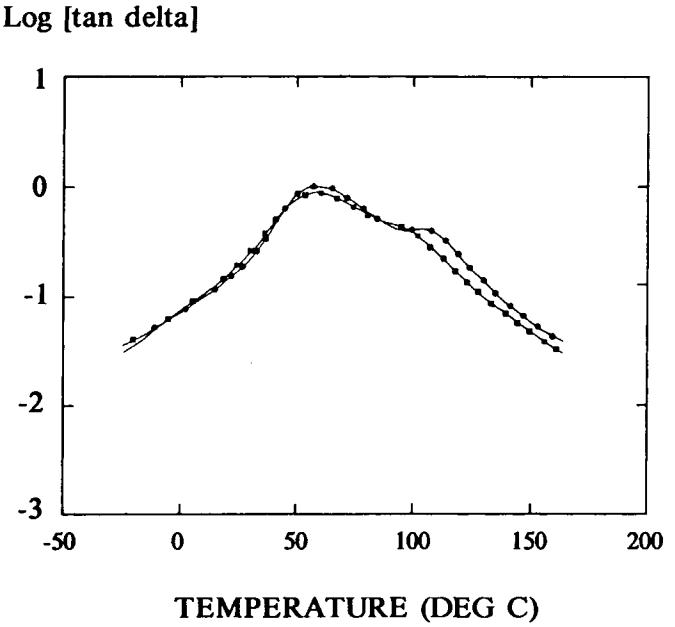

Figure 16 Effect of swelling and polymerization temperature on tan σ of composite sample while fixing PS particle content and crosslink density. (●): C-PS(1)/PBMA(2)-15/85-40; (■): C-PS(1)/PBMA(2)-15/85-0.

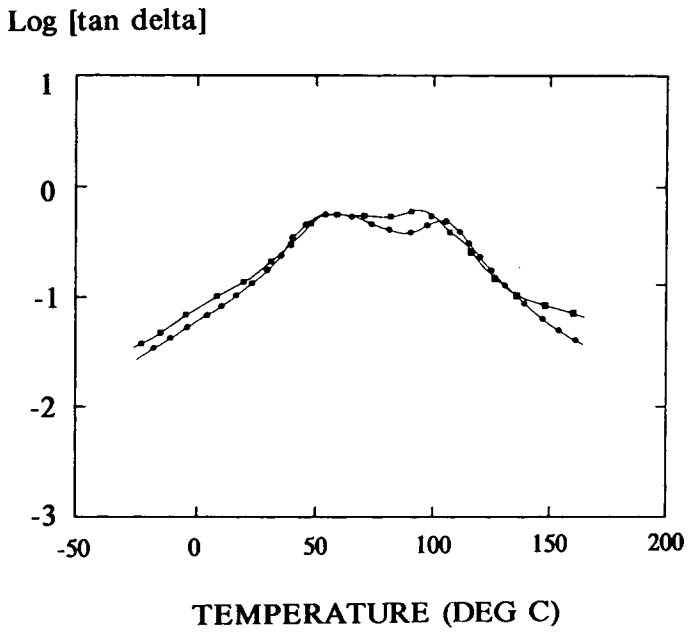

Figure 17 Effect of swelling and polymerization temperature on tan delta of composite sample while fixing PS particle content and crosslink density. (●): C-PS(1)/PBMA(2)-25/75-40; (■): C-PS(1)/PBMA(2)-25/75-0.

position. The PS transition peaks show a significant shift toward lower temperature when it is synthesized at a lower temperature, while the position of the PBMA transition remains constant. In order to check if this difference is caused by the difference in the structure of PBMA matrix network polymerized at different temperatures, PBMA homonetworks synthesized at 0°C and 40°C are charac-

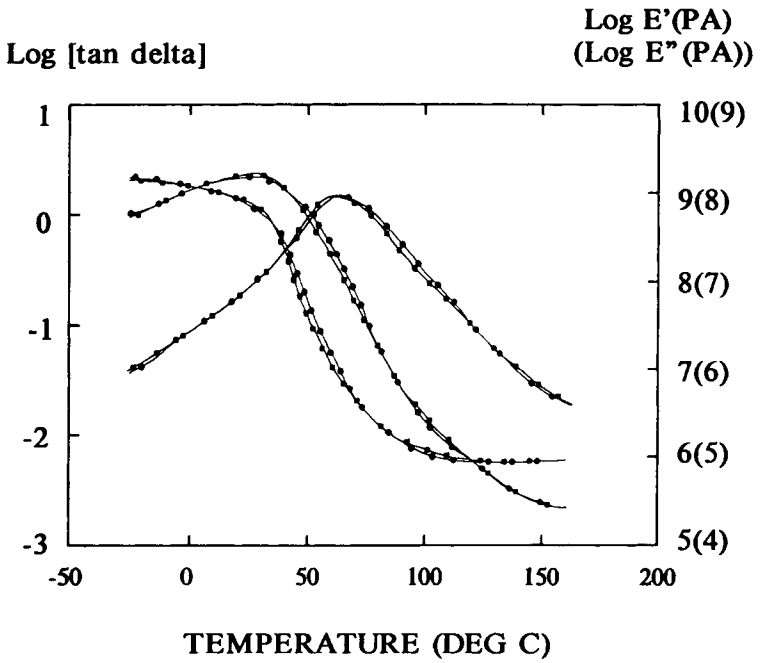

Figure 18 Tan delta and modulus behaviour of PBMA homonetwork synthesized at 0°C and 40°C. (●): H-PBMA(2)-40; (■): H-PBMA(2)-0.

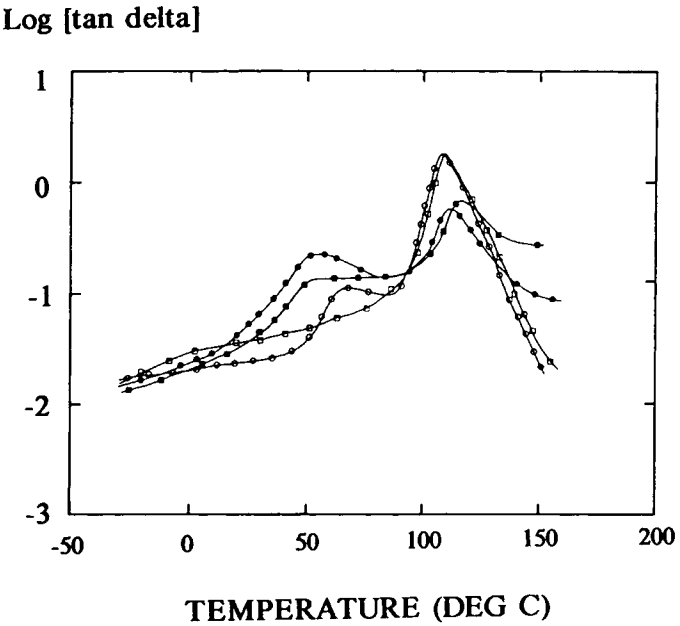

Figure 19 Effect of polymerization temperature in bulk IPN samples. (●): B-PS(1)/PBMA(2)-40; (○): B-PS(1)/PBMA(2)-0; (■): B-PS(2)/PBMA(2)-40; (□): B-PS(2)/PBMA(2)-0.

terized. It is found that the difference in polymerization temperature does not result in a noticeable change (Fig. 18).

In seeking the possible cause of such a shift, the tan δ spectra of bulk IPN synthesized at two different temperatures are characterized as shown in Figure 19. Regardless of the crosslink density of the polystyrene phase, inward shifts of both PS and PBMA transitions are observed for the 0°C polymerized sample relative to that of the 40°C one,

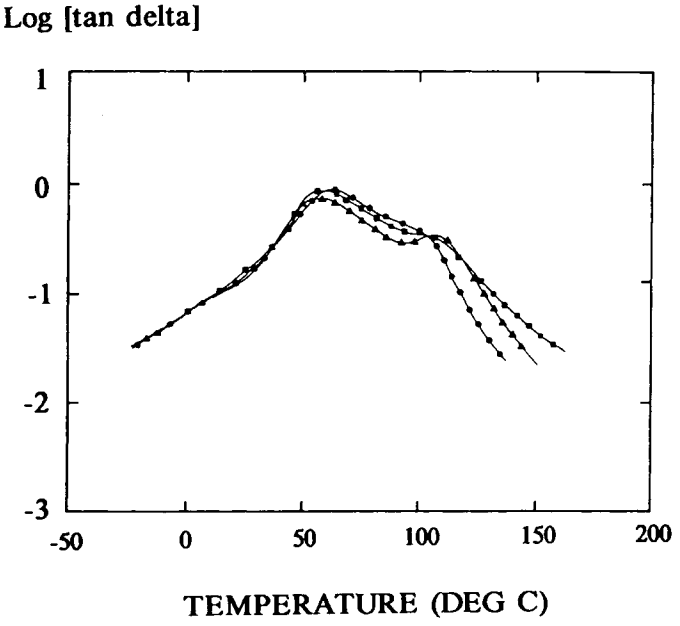

Figure 20 Effect of PS particle size on tan δ of composite sample. (●): C-PS(1″)/PBMA(2)-40, 1.3 μm; (■): C-PS(1)/PBMA(2)-40, 0.5 μm; (▲): C-PS(1′)/PBMA(2)-40, 0.17 μm.

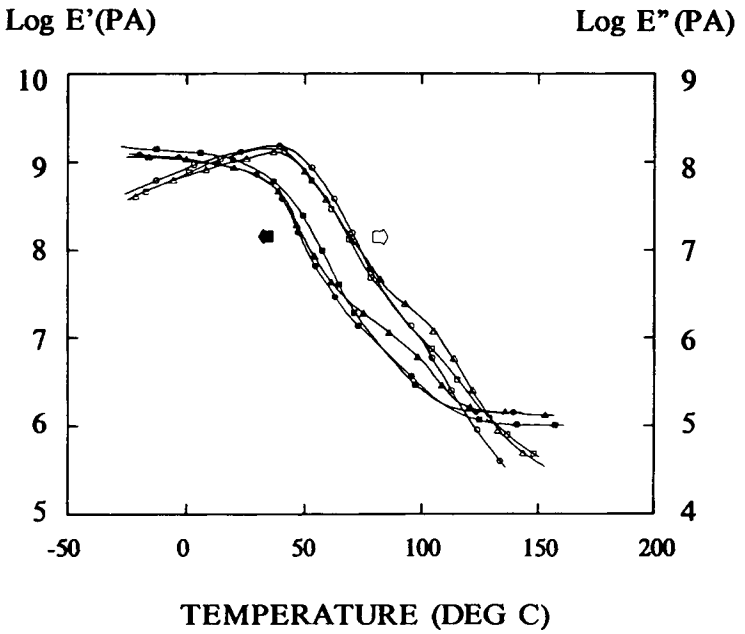

Figure 21 Effect of PS particle size on modulus of composite sample. (●): C-PS(1")/PBMA(2)-40, 1.3 μm; (■): C-PS(1)/PBMA(2)-40, 0.5 μm; (▲): C-PS(1')/PBMA(2)-40, 0.17 μm.

which is indicative of better miscibility between components in the 0°C sample relative to the 40°C sample. Therefore, the downshift of tan δ of the 0°C to that of the 40°C composite sample can be considered to be a consequence of the better miscibility in the former sample. However, in composite samples, no noticeable shift of PBMA transition was observed. This may be a consequence of the fact that the major portion of the PBMA fraction is located outside of the PS network's influence as continuous phase and does not have a chance to interact molecularly with PS networks.

Effect of PS Particle Size

In this case, fixing overall composition, crosslink density of each component, and temperature, the size of particles was varied from 0.17 to 1.3 micron. Figure 20 compares the tan δ of three samples with different PS particle sizes. The sample containing the largest particle size indicates the most significant inward shift of PS and PBMA transitions. The storage and loss modulus behaviour also show considerable difference among samples especially in the vicinity of PS transition region (Fig. 21). Recalling that the change in the effective volume fraction of the dispersed phase, while fixing the properties of the dispersed domain, does not cause any noticeable change (Fig. 4), this is a rather unexpected result since the only difference among the samples is the size of complex domains and the properties of individual complex domains is not varied. In usual hard particulate-filled polymer, the degree of interaction between filler and matrix is known to be dependent on the surface area to volume ratio of filler. Thus, it is increased as the particle size is decreased if compared at the same loading. Therefore, it is less likely that the difference in the size of PS particles causes such shifts. Consequently, it can be speculated that the shifts observed in this series of samples might be related to factors other than surface to volume ratio or changes in the properties of the dispersed domain itself, such as the overall arrangement of dispersed and continuous phase.

CONCLUSIONS

Among the various experimental and material factors affecting the dynamic mechanical behaviour of polymeric composites with complex dispersed phase, the volume fraction and the properties of individual dispersed domains have been varied, either by changing the crosslink density or by using different sample preparation schemes. Their effects have been evaluated.

The height of the tan δ peak of each phase is found to be generally dependent on the effective

volume fraction of the dispersed phase composed of PS and PBMA occlusion rather than on the overall composition as suggested in many previous studies.

The increase in the crosslink density of PS particles is directly reflected in the tan δ behaviour of a composite sample as a shift toward higher temperature. When the effective volume of dispersed phase is controlled by changing the temperature of swelling and polymerization, the peak position of PS tan δ is found to shift to lower temperature with a decrease in the sample preparation temperature, indicating better miscibility between PS and PBMA. This observation is substantiated by the tan δ behavior of bulk IPN samples synthesized at different temperatures.

Comparisons among composite, homonetworks, and bulk IPN sample (which is expected to have identical structure to that of the dispersed domain in the composite sample) suggest that the peak position of tan δ is also affected by morphological characteristics such as continuity of phase. The change in the size of PS particles results in rather significant variations in the PS tan δ position. While the detailed cause of such variation cannot be addressed at this moment, this point is the subject of further investigation.

The authors are pleased to thank the Korea Science and Engineering Foundation for financial support.

REFERENCES

1. J. D. Keitz, J. W. Barlow, and D. R. Paul, *J. Appl. Polym. Sci.*, **29,** 3131 (1984).
2. J. Y. Cavaille, J. Perez, C. Jourdan, and G. P. Johari, *J. Polym. Sci. Polym. Phys.*, **25,** 1847 (1987).
3. J. K. Yeo, L. H. Sperling, and D. A. Thomas, *Polym. Eng. Sci.*, **21,** 696 (1981).
4. J. A. Manson and L. H. Sperling, *Polymer Blends and Composites,* Plenum Press, New York, 1976.
5. F. S. Bates, R. E. Cohen, and A. S. Argon, *Macromolecules,* **16,** 1108 (1983).
6. P. S. Theocaris and G. D. Spathis, *J. Appl. Polym. Sci.*, **27,** 3019 (1982).
7. G. Kraus and K. W. Rollmann, *J. Polym. Sci. Polym. Phys.*, **14,** 1133 (1976).
8. R. D. Corsaro and L. H. Sperling, Eds., *Sound and Vibration Damping with Polymers,* ACS Symposium Series **424,** ACS, Washington D.C., 1990.
9. D. Klempner, C. L. Wang, M. Ashitiani, and K. C. Frisch, *J. Appl. Polym. Sci.*, **32,** 4197 (1986).
10. J. K. Yeo, L. H. Sperling, and D. A. Thomas, *Polym. Eng. Sci.*, **22,** 190 (1982).
11. D. J. Hourston, R. Satgurunathan, and H. C. Varma, *J. Appl. Polym. Sci.*, **34,** 901 (1987).
12. K. W. McLaughlin, *Polym. Eng. Sci.*, **299,** 1580 (1989).
13. H. L. Frisch, D. Klempner, H. K. Yoon, and K. C. Frisch, *Macromolecules,* **13,** 1016 (1980).
14. A. R. Schultz and B. M. Beach, *Macromolecules,* **7,** 902 (1974).
15. S. A. Paipetis, *Colloid Polym. Sci.*, **258,** 42 (1980).
16. K. Isaka and K. Shibayama, *J. Appl. Polym. Sci.*, **22,** 1321 (1978).
17. M. Kodama and I. Karino, *J. Appl. Polym. Sci.*, **32,** 5057 (1986).
18. M. Kodama and I. Karino, *J. Appl. Polym. Sci.*, **32,** 5345 (1986).
19. T. Kunori and P. H. Geil, *J. Macro. Sci.-Phys.*, **B18,** 93 (1980).
20. B. Gregory, A. Hiltner, and E. Baer, *Polym. Eng. Sci.*, **27,** 568 (1987).
21. J. L. Gomez Ribelles, J. Mano Sebastia, R. Marti Soler, M. Monleon Pradas, A. Ribes Greus, and J. J. Suay Anton, *J. Appli. Polym. Sci.*, **42,** 1647 (1991).
22. L. E. Nielsen, *Polym. Eng. Sci.*, **17,** 713 (1977).
23. E. H. Kerner, *Proc. R. Soc. (London),* **B69,** 808 (1956).
24. L. E. Nielsen, *J. Appl. Polym. Sci.*, **14,** 4626 (1976).
25. J. C. Halpin and J. L. Kardos, *Polym. Eng. Sci.*, **16,** 344 (1976).
26. J. Y. Cavaille, C. Jourdan, X. Z. Kong, J. Perez, C. Pichot, and J. Guillot, *Polymer,* **27,** 693 (1986).
27. C. Jourdan, J. Y. Cavaille, and J. Perez, *Polym. Eng. Sci.*, **28,** 1318 (1988).
28. M. J. Guest and J. H. Daly, *Eur. Polym. J.*, **26,** 603 (1990).
29. R. A. Dickie, *J. Appl. Polym. Sci.*, **17,** 45 (1973).
30. E. R. Wagner and L. M. Robeson, *Rubber Chem. Technol.*, **43,** 1129 (1970).
31. G. Cigna, *J. Appl. Polym. Sci.*, **14,** 1781 (1970).
32. A. A. Donatelli, L. H. Sperling, and D. A. Thomas, *Macromolecules,* **9,** 671 (1976).
33. V. Huelck, D. A. Thomas, and L. H. Sperling, *Macromolecules,* **5,** 348 (1972).
34. L. H. Sperling, *Interpenetrating Polymer Networks and Related Materials,* Plenum Press, New York, 1981.
35. L. Bohn, *Angew. Makromol. Chem.*, **20,** 129 (1971).
36. L. Marbitzer, K. Ott, M. Schuster, and D. Kranz, *Angew. Makromol. Chem.*, **7,** 57 (1972).
37. F. S. Bates, R. E. Cohen, and A. S. Argon, *Macromolecules,* **16,** 1108 (1983).